

Low-frequency noise and linearity of a $\text{YBa}_2\text{Cu}_3\text{O}_7$ dc superconducting quantum interference device magnetometer in static magnetic fields

S. Krey,^{a)} H.-J. Barthelmeß, and M. Schilling

Universität Hamburg, Institut für Angewandte Physik und Zentrum für Mikrostrukturforschung,
Jungiusstraße 11, D-20355 Hamburg, Germany

(Received 21 May 1999; accepted for publication 31 August 1999)

We have investigated the low-frequency noise and effective flux sensing area of a field cooled dc superconducting quantum interference device magnetometer from $\text{YBa}_2\text{Cu}_3\text{O}_7$ in magnetic fields up to $200 \mu\text{T}$, both before and after it was patterned with holes to reduce the maximum structural width of the pickup loop. We find that even in low fields the noise of the unpatterned magnetometer steadily increases with the applied field. However, after the patterning for the holes, the noise remains at the zero field level up to a threshold field of $35 \mu\text{T}$ and is always less than in the unpatterned case. This threshold field is also found in field dependent measurements of the total harmonic distortion. The effective area of the magnetometer depends on the cooling field, and the dependence is different in the unpatterned and the patterned case. © 1999 American Institute of Physics. [S0021-8979(99)05523-1]

A severe obstacle for many practical applications of dc superconducting quantum interference device (SQUID) magnetometers from high temperature superconductors (HTSs) has long been the increase of low-frequency noise when the magnetometer is operated in an ambient magnetic field, like the earth's field of about $50 \mu\text{T}$. This excess noise is caused by the thermally activated random hopping of magnetic flux vortices between their pinning sites.¹ The vortices are either created when the magnetometer is cooled below its critical temperature T_c in an ambient field, or they are introduced into the film by the Lorentz force from shielding currents.² The spectral density S_Φ of the flux noise typically scales with $1/f$ as a function of the frequency f and therefore adversely affects low-frequency applications like biomagnetism or geophysical measurements. Since the number of vortices is proportional to the cooling field B_0 , S_Φ is expected to scale linearly with B_0 . Moreover, the amount of noise is strongly dependent on the epitaxial quality of the involved superconducting thin films.^{3,4} Noise measurements depending on the applied field have been reported for bare dc SQUIDs,^{5,6} directly coupled magnetometers,^{5,7-9} rf SQUIDs,^{10,11} and magnetometers from HTS multilayers.¹²

Recently, Dantsker *et al.*^{13,14} made several suggestions for the design of HTS SQUID devices in order to reduce the amount of trapped flux. They are based on the reduction of the linewidth of the SQUID body, so that it becomes energetically unfavorable for flux to enter the film. An estimation for the threshold field of flux entry is given by $B_T = \pi\Phi_0/4w^2$, where w is the linewidth of the film. Bare SQUIDs with slots or holes and linewidths of $4 \mu\text{m}$ showed no excess noise in cooling fields up to about $100 \mu\text{T}$. Cho *et al.*⁹ repatterned the pickup loop of a complete directly coupled magnetometer to obtain a mesh of $4 \mu\text{m}$ wide lines.

However, they found a major noise contribution from the tapered outer edges of their magnetometers. After their removal, the low-frequency noise remained constant again in cooling fields below $100 \mu\text{T}$, and no further effect from the mesh pattern was observed. This is attributed to the narrow linewidth of their SQUID loop and the large inductance mismatch between pickup loop and SQUID.

Here, we present noise measurements on a similar directly coupled magnetometer, both before and after it was patterned with holes to reduce the maximum structural width of the pickup loop. We directly compare the effects of this kind of patterning for the same device, since the comparison of different devices may be misleading, because of a variable microstructural or epitaxial quality of the involved superconducting thin films. Besides the low-frequency noise, further aspects become important when considering the unshielded operation of a HTS magnetometer system. One important issue is the linearity of the system, since small signals have to be resolved at a high level of ambient noise. To characterize the magnetometer linearity, we measured the total harmonic distortion (THD) in different cooling fields. Furthermore, we investigate the dependence of the effective flux sensing area on the cooling field.

Our directly coupled dc SQUID magnetometers are prepared from a single epitaxial $\text{YBa}_2\text{Cu}_3\text{O}_7$ thin film on a symmetrical (100) SrTiO_3 bicrystal with 24° misorientation angle. We typically use films of 120 nm thickness, which are deposited by KrF excimer laser deposition. After the patterning with conventional photolithography and argon plasma etching, the magnetometers are treated in an oxygen plasma. Finally, the contact pads are covered with silver to reduce the contact resistance. The magnetometer layout is similar to the one introduced by Lee *et al.*¹⁵ with a washer-type pickup loop of an outer dimension of 8.3 mm and an inner hole size of $3 \times 3 \text{ mm}^2$. The SQUID loop has an outer area of $16 \times 56 \mu\text{m}^2$ and an inner hole of $4 \times 50 \mu\text{m}^2$, from which we

^{a)}Electronic mail: krey@physnet.uni-hamburg.de

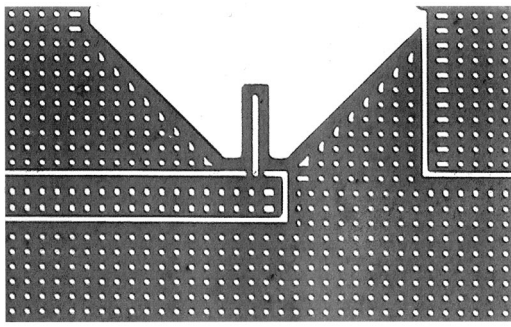


FIG. 1. Micrograph of the magnetometer part around the SQUID loop after it was completely patterned with holes. The holes have a diameter of about $4 \mu\text{m}$ and the linewidth between them is about $5.2 \mu\text{m}$.

calculate a SQUID inductance of 60 pH, including the kinetic contribution. The bicrystal junctions are nominally $3 \mu\text{m}$ wide. After the first characterization of the magnetometer with solid pickup loop, it was patterned a second time using a net-like photomask. We obtained a linewidth of about $5.2 \mu\text{m}$ and circular holes with a diameter of about $4 \mu\text{m}$ across the whole pickup loop. Figure 1 depicts a micrograph of the region around the SQUID loop after the patterning.

All measurements were performed in liquid nitrogen inside of a triple mumetal shield. The magnetic field B_0 was applied with a Helmholtz coil that was supplied by a large capacity lead-acid battery and an appropriate resistor. The flux density noise, resulting from the current noise in the coil, is less than $85 \text{ fT}/\sqrt{\text{Hz}}$ at 3 Hz and $B_0 = 100 \mu\text{T}$, and does not significantly contribute to the measured noise values. The noise measurements were made in flux-locked-loop (FLL) mode with bias current reversal to reject the low-frequency noise from critical current fluctuations in the junctions. In all field dependent measurements, the magnetic field was applied while the magnetometer was heated above T_c , and it remained on during the cooling and the measurements. Hence, no shielding currents were generated as in a switching process. The magnetometer properties in the zero field cooled case, before and after the second patterning step for the holes, are listed in Table I. After the treatment, I_0 and R_n were somewhat changed, presumably due to a slight oxygen loss in the junctions, since no second plasma oxidation was carried out. Surprisingly, the patterning had only a minor effect on the sensitivity of the device. The effective area increased by about 2%, although the character of input coupling completely changed. With the solid pickup loop, flux is

TABLE I. Transport properties of the investigated magnetometer at $T = 77 \text{ K}$ in zero external magnetic field, before and after the patterning.

		Before	After	
Voltage swing	ΔV	26	27	μV
Critical current ^a	I_0	107	76.5	μA
Normal resistance ^a	R_n	2.1	2.8	Ω
Sensitivity	B/Φ	9.203	8.980	nT/Φ_0
Effective area	$A_{\text{eff}} = \Phi/B$	0.225	0.230	mm^2

^aValues given per junction.

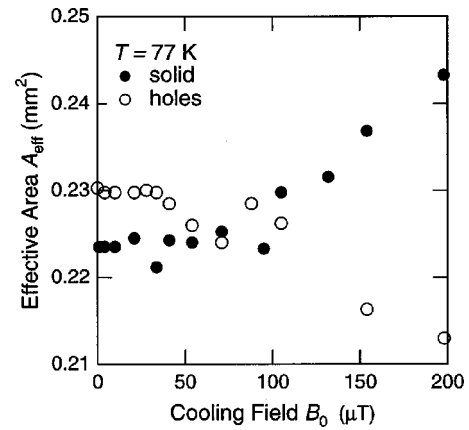


FIG. 2. Effective area depending on the cooling field for the unpatterned (solid) and the patterned (holes) magnetometer.

focused to some extent into the loop by the Meissner effect. In the patterned device, however, this effect is replaced by the flux quantization, which keeps the flux in the holes constant at integer flux quanta. Thus, flux changes must be partly focused into the pickup loop, again. Obviously, there is no significant quantitative difference between both effects in zero field. However, a difference is found in field dependent measurements, whose results are depicted in Fig. 2. For the solid device, we find an increase of the effective area above roughly $B_0 = 100 \mu\text{T}$, whereas it is a decrease with nearly the same variation for the patterned device above $35 \mu\text{T}$. Hence, the sensor's calibration is affected by larger cooling fields. This is an important issue for the design of multichannel biomagnetic systems intended for unshielded operation, since their signal processing demands an exact knowledge of each sensor's effective area, but this is usually measured inside a shield. The effect is small for the earth's magnetic field, but it might be larger for a different magnetometer layout. The reason for the dependence of the effective area on the cooling field is not yet clear and is under further investigation.

Figure 3 depicts several flux density noise spectra for the unpatterned magnetometer in different cooling fields B_0 . We find an increasing low-frequency noise with B_0 from the growing number of trapped vortices in the film. The spectra for $B_0 = 41$ and $198 \mu\text{T}$ include a Lorentzian contribution, caused by the random telegraph signal (RTS) from a predominant two-level fluctuator. Figure 4(a) shows the noise values at the frequency 3 Hz depending on B_0 , before and after the holes were patterned into the pickup loop. In the unpatterned case, the low-frequency noise increases with B_0 even for the lowest cooling fields, whereas it remains approximately constant below a threshold field $B_T \approx 35 \mu\text{T}$ in the patterned case. Moreover, we find, that for all values of B_0 , the magnetometer with holes remains markedly less noisy than with solid pickup loop. In the unpatterned case, the noise below B_T presumably results from the motion of vortices near the SQUID loop, which is directly coupled into the SQUID, since the indirect component from noise currents in the pickup loop is strongly suppressed by the poor coupling between the inductances of the pickup loop and the SQUID.⁹ In both cases, we observed a significant increase of

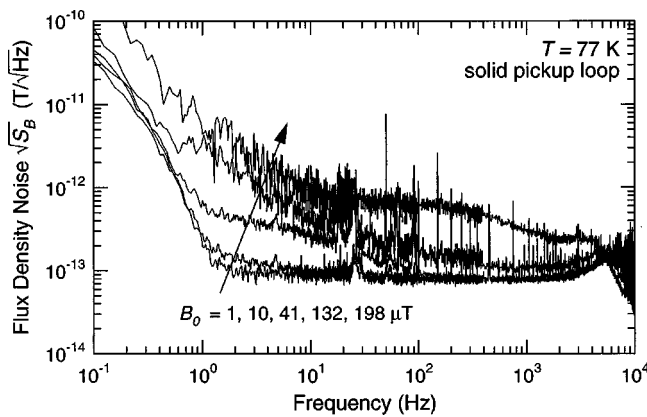


FIG. 3. Flux density noise spectra of the unpatterned magnetometer for different cooling fields B_0 .

noise above B_T . We attribute this to flux entry into the SQUID loop, although a somewhat larger threshold field of $42 \mu\text{T}$ for the measured width $w = 6.2 \mu\text{m}$ is expected. In particular in the unpatterned case, the noise values above the threshold field remain on a nearly constant level up to $B_0 \approx 80 \mu\text{T}$. This noise was caused by the dominating RTS from a single fluctuator and therefore does not scale with B_0 . For higher values of B_0 , it is covered by the noise of the remaining vortices.

Nonlinear behavior of a SQUID magnetometer can result from the inelastic motion of vortices in the magnetometer body.¹⁶ Thus, the degree of nonlinearity is expected to

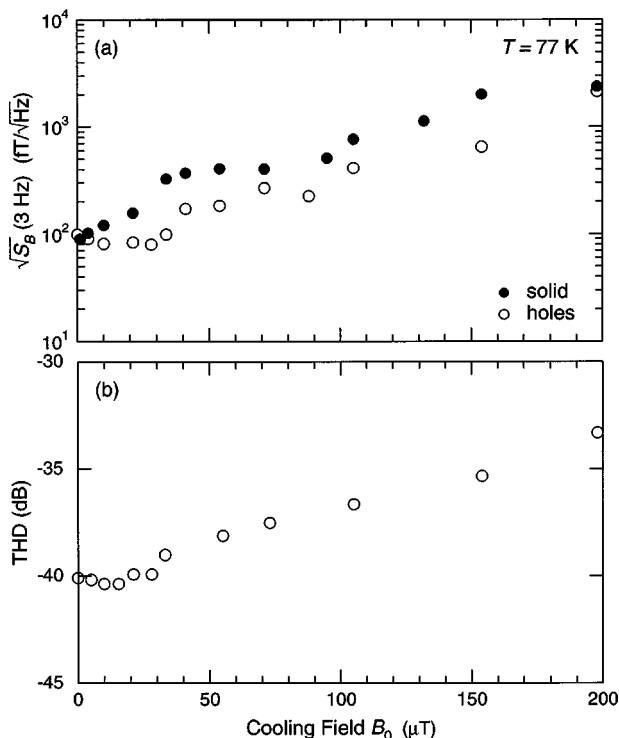


FIG. 4. (a) Flux density noise at 3 Hz vs cooling field for the directly coupled magnetometer, before (●) and after it was completely patterned with holes (○). (b) Total harmonic distortion (THD) of the patterned magnetometer depending on the cooling field.

depend on the number of vortices and on the cooling field. To measure the magnetometer linearity, we applied a sinusoidal magnetic test signal with a peak-to-peak amplitude of 20 nT and the frequency $f = 518 \text{ Hz}$. The output voltages from the signal source and the FLL electronics were electronically subtracted to obtain a maximum suppression of the harmonics of the test signal. The residual signal was measured with a spectrum analyzer. Figure 4(b) shows the amount of THD of the patterned magnetometer depending on the cooling field. The THD values show a very similar dependence on B_0 as is found in the noise measurements. The THD remains nearly constant for fields below a threshold and increases for cooling fields beyond this value, whereby the threshold field agrees well with the value found in the noise measurements.

In conclusion, we have confirmed the results of Dantsker and co-workers for a practical HTS SQUID magnetometer of high sensitivity. The noise of a field cooled directly coupled magnetometer can be significantly lowered by reducing its maximum linewidth through holes in the pickup loop. The observed threshold field is attributed to flux entry into the SQUID loop, which should be made narrower in future layouts. The patterning has little effect on the zero field cooled effective area of the device. However, we found that the effective area depends on the cooling field, and that the dependence is different before and after the patterning. This is under further investigation. The linearity of the magnetometer is also affected by cooling fields above the threshold field. The measured THD values show a similar dependence on the cooling field as the low-frequency noise.

This work was supported by the German BMBF under Contract No. 13N7323-8.

- ¹M. J. Ferrari *et al.*, Phys. Rev. Lett. **64**, 72 (1990).
- ²J. Z. Sun, W. J. Gallagher, and R. H. Koch, Phys. Rev. B **50**, 13664 (1994).
- ³M. J. Ferrari, M. Johnson, F. C. Wellstood, J. Clarke, P. A. Rosenthal, R. H. Hammond, and M. R. Beasley, Appl. Phys. Lett. **53**, 695 (1988).
- ⁴R. Scharnweber, N. Dieckmann, and M. Schilling, Appl. Phys. Lett. **70**, 2189 (1997).
- ⁵A. H. Miklich *et al.*, Appl. Phys. Lett. **64**, 3494 (1994).
- ⁶M. I. Faley, U. Poppe, K. Urban, H. Hilgenkamp, H. Hemmes, W. Aarnink, J. Flokstra, and H. Rogalla, Appl. Phys. Lett. **67**, 2087 (1995).
- ⁷R. H. Koch, J. Z. Sun, V. Foglietta, and W. J. Gallagher, Appl. Phys. Lett. **67**, 709 (1995).
- ⁸F. P. Milliken, S. L. Brown, and R. H. Koch, Appl. Phys. Lett. **71**, 1857 (1997).
- ⁹H.-M. Cho, R. McDermott, B. Oh, K. A. Kouznetsov, A. Kittel, J. H. Miller, Jr., and J. Clarke, IEEE Trans. Appl. Supercond. **9**, 3294 (1999).
- ¹⁰C. P. Foley, S. Lam, K. E. Leslie, K.-H. Müller, R. A. Binks, L. Macks, and G. J. Sloggett, Proceedings of the 6th International Superconductive Electronics Conference (ISEC'97), Berlin, June 25–28, 1997.
- ¹¹J. Borgmann, P. David, R. Otto, J. Schubert, and A. I. Braginski, Appl. Phys. Lett. **74**, 1021 (1999).
- ¹²S. Krey, B. David, R. Eckart, and O. Dössel, Appl. Phys. Lett. **72**, 3205 (1998).
- ¹³E. Dantsker, S. Tanaka, P.-Å Nilsson, R. Kleiner, and J. Clarke, Appl. Phys. Lett. **69**, 4099 (1996).
- ¹⁴E. Dantsker, S. Tanaka, and J. Clarke, Appl. Phys. Lett. **70**, 2037 (1997).
- ¹⁵L. P. Lee, J. Longo, V. Vinetskiy, and R. Cantor, Appl. Phys. Lett. **66**, 1539 (1995).
- ¹⁶R. H. Koch, M. B. Ketchen, W. J. Gallagher, R. L. Sandstrom, A. W. Kleinsasser, D. R. Gambrel, T. H. Field, and H. Matz, Appl. Phys. Lett. **58**, 1786 (1991).